Inorganic Chemistry

Article

Synthesis and Characterization of Diverse Coordination Polymers. Linear and Zigzag Chains Involving Their Structural Transformation via Intermolecular Hydrogen-Bonded, Interpenetrating Ladders Polycatenane, and Noninterpenetrating Square Grid from Long, Rigid *N,N′*-Bidentate Ligands: 1,4-Bis[(*x*-pyridyl)ethynyl]benzene (*x* = 3 and 4)

Md. Badruz Zaman,*,† Konstantin Udachin, and John A. Ripmeester*

Steacie Institute for Molecular Science, National Research Council Canada, Ottawa, Ontario K1A 0R6, Canada

Mark D. Smith and Hans-Conrad zur Loye

Department of Chemistry and Biochemistry, University of South Carolina, Columbia, South Carolina 29208

Received January 18, 2005

The long, rigid ligands 1,4-bis[(3-pyridyl)ethynyl]benzene (**L1**) and 1,4-bis[(4-pyridyl)ethynyl]benzene (**L2**) were used in the synthesis of 10 new organic–inorganic coordination frameworks, each of them adopting different structural motifs. Synthesis, single-crystal X-ray structure determination, and spectroscopic and thermogravimetric analyses are presented. The reactions between $M(NO_3)_2 \cdot xH_2O$; M = Cd(II), Cu(II), and Co(II); $x = 3$–6 and $Cu(hfac)_2 \cdot H_2O$ [hfac = bis(hexafluoroacetylacetonato)] with **L1** afforded the following one-dimensional zigzag chain structures: $[Cd(C_{20}H_{12}N_2)_{0.5}(NO_3)(CH_3OH)]_n$ (**1**, monoclinic, *C2/c*; $a = 7.586(1)$ Å, $b = 23.222(1)$ Å, $c = 13.572(1)$ Å, $\beta = 92.824(1)$, $Z = 4$); $[\{Cu(C_{20}H_{12}N_2)(NO_3)_2(CH_3OH)\} \cdot CH_3OH]_n$ (**2**, orthorhombic, $P2_12_12_1$; $a = 8.589(1)$ Å, $b = 15.766(1)$ Å, $c = 17.501(1)$ Å, $Z = 4$); $[Co(C_{20}H_{12}N_2)_2(NO_3)_2(H_2O)_2]$ (**5**, triclinic, $P\bar{1}$; $a = 7.493(1)$ Å, $b = 8.948(1)$ Å, $c = 14.854(1)$ Å, $\alpha = 100.427(1)$, $\beta = 97.324(1)$, $\gamma = 110.901(1)$, $Z = 1$); $[Cu(C_{20}H_{12}N_2)(hfac)_2]_n$ (**4**, monoclinic, *C2/c*, $a = 18.828(1)$ Å, $b = 14.671(1)$ Å, $c = 13.427(1)$ Å, $\beta = 90.447(1)°$, $Z = 4$). Moreover, the minority phase compound formed from $Cu(NO_3)_2 \cdot 3H_2O$ and **L1** yielded a metallocyclic chain structure, $[Cu(C_{20}H_{12}N_2)(NO_3)]_n$ (**3**, triclinic, $P\bar{1}$; $a = 8.728(1)$ Å, $b = 10.018(1)$ Å, $c = 11.893(1)$ Å, $\alpha = 109.991(1)$, $\beta = 97.109(1)$, $\gamma = 115.542(1)$, $Z = 1$). In addition to the dinuclear coordination complex **5**, all other polymeric structures (**1**–**4**) from **L1** are composed of interpenetrating 2D and 3D cross-linked zigzag chains via hydrogen-bonding interactions. The reactions between $M(NO_3)_2 \cdot xH_2O$; M = Cd(II), Cu(II), and Co(II); $x = 3$–6 and $Cu(hfac)_2 \cdot H_2O$ [hfac = bis(hexafluoroacetylacetonato)] and **L2** were dependent on the nature of the metal center and resulted in the formation of four different interpenetrating and noninterpenetrating compounds (**6**–**10**): $[Co(C_{20}H_{12}N_2)_{1.5}(NO_3)_2]_n$ (**6**, triclinic, $P\bar{1}$; $a = 14.172(1)$ Å, $b = 15.795(1)$ Å, $c = 18.072(1)$ Å, $\alpha = 115.380(1)$, $\beta = 101.319(1)$, $\gamma = 93.427(2)$, $Z = 4$), which consists of T-shaped building blocks assembled into three-dimensional interpenetrating polycatenated ladders; $[Cd(C_{20}H_{12}N_2)_2(NO_3)_2]_n$ (**7**, monoclinic, *I2/a*; $a = 11.371(1)$ Å, $b = 20.311(2)$ Å, $c = 15.240(2)$ Å, $\beta = 100.201(2)°$, $Z = 4$), which adopts a two-dimensional noninterpenetrating square-grid motif; $[Cu(C_{20}H_{12}N_2)(hfac)_2]_n$ (**8**, monoclinic, *I2/a*; $a = 11.371(1)$ Å, $b = 20.311(2)$ Å, $c = 15.240(2)$ Å, $\beta = 100.201(2)°$, $Z = 4$), composed of three sets of distinct one-dimensional linear chains; $[Cu(C_{20}H_{12}N_2)(EtOH)(NO_3)_2][Cu(C_{20}H_{12}N_2)_{1.5}(NO_3)_2] \cdot 2EtOH$ (**9**, triclinic, $P\bar{1}$; $a = 12.248(2)$ Å, $b = 13.711(3)$ Å, $c = 18.257(4)$ Å, $\alpha = 108.078(4)°$, $\beta = 97.890(4)°$, $\gamma = 103.139(5)°$, $Z = 2$) and $[Cu(C_{20}H_{12}N_2)(MeOH)(NO_3)_2][Cu(C_{20}H_{12}N_2)_{1.5}(NO_3)_2] \cdot 2MeOH$ (**10**, triclinic, $P\bar{1}$; $a = 12.136(1)$ Å, $b = 13.738(2)$ Å, $c = 17.563(3)$ Å, $\alpha = 107.663(3)°$, $\beta = 94.805(4)°$, $\gamma = 104.021(4)°$, $Z = 2$). Both **9** and **10** stack into infinite interpenetrating ladders through bundles of infinite chains and are described in our preliminary communication.

Introduction

Construction of supramolecular systems composed of long, rigid, and conjugated bridging molecules with pyridyl

substituents at the terminal positions are expected to afford interesting supramolecular architectures by intermolecular

---

* Authors to whom correspondence should be addressed. E-mail: john.ripmeester@nrc.ca (J.A.R.); zaman@emt.inrs.ca (M.B.Z.).

† Present address: Institut National de la Recherche Scientifique, Centre Énergie, Matériaux et Télécommunications, 1650 Bd. Lionel-Boulet, Varennes, Quebec J3X 1S2, Canada.

interactions such as hydrogen bonding[1−5] and coordination with metals.[3−14] Supramolecular species formed by self-assembly exhibit interesting properties such as luminescence,[14−19] redox activity,[14,18−21] and magnetism.[14,22−25] Moreover, such molecules have also attracted much attention because of their potential use as alligator clips for the development of molecular wires.[26−28]

In the dipyridyl compounds, the structures and properties can be modified by changing the nitrogen positions and spacer groups.[28,29] We have found that dipyridyl acetylenes assemble into one-dimensional supramolecular tapes by hydrogen-bonding complexation with chloranilic acid, whose supramolecular structures and electronic states are strongly dependent on the nitrogen positions.[29] The nitrogen positions in the dipyridyl compounds also modify the metal−ligand coordination environments that can also be influenced by judicious choice of the metal center. We have recently reported the synthesis and structural characterization of organic/inorganic coordination polymers composed of N,N'-dipyridylacetylene ($N,N' = 2, 3, 4$) ligands and metal(II) nitrate/metal(II) hexafluoroacetyl-acetonate salts (metal = Cu, Mn, Zn).[30] In addition, we characterized a variety of their respecting structural features, ranging from sinusoidal and zigzag chains to two-dimensional interpenetrating channel-type architectures.[31−33] Furthermore, N,N'-dipyridylbutadiyne ($N,N' = 2, 3, 4$) ligands have often been reported to assemble into interesting supramolecular structures.[33,34] In this context, we have introduced a benzene ring into the skeleton of N,N'-dipyridylbutadiyne: 1,4-bis[(x-pyridyl)ethynyl]benzene; $x = 3$ (**L1**), 4 (**L2**).[35] There are numerous advantages in the introduction of these *long, rigid* ligands: First, the benzene ring increases the length and diameter of these ligands, perhaps allowing control of the physical dimensions of the crystalline architecture and thereby allowing control of the internal chemistry of the coordination polymers. Such linkers may inhibit interpenetration and enable the formation of large macrocyclic compounds with infinite channels.[10,36] Second, compounds containing benzene with acetylene linkages may increase the polarization properties that are expected to afford well-ordered intermolecular interactions. The acetylene-conjugated molecules are also of interest from the viewpoint of fluorescent behavior for electroluminescence devices.[35,37] Third, the chemical nature of the long ligands provides a tendency to form T-joint building blocks with metal centers,[32,38−44] which may give rise to several isomeric framework architectures. Our newly designed Schiff-base ligands [1,4-bis(x-pyridyl)-2,3-diaza-1,3-butadienes; $x = 2$, 3, 4] have already been demonstrated to serve as T-joint building blocks for use in assembly of a wide variety of new coordination polymers.[32,43,44] In general, the polymer topology generated in these systems can be controlled by the judicious choice of organic ligands that contain two pyridyl donor units

(1) Zaman, M. B.; Tomura, M.; Yamashita, Y. *J. Org. Chem.* **2001**, *66*, 5987−5995.

(2) Felloni, M.; Blake, A. J.; Hubberstey, P.; Wilson, C.; Schroder, M. *CrystEngComm* **2002**, *4*, 483−495.

(3) Aakeroy, C. B.; Beatty, A. M.; Leinen, D. S. *Angew. Chem., Int. Ed.* **1999**, *38*, 1815−1819.

(4) Recent review for hydrogen bonded networks of coordination complexes: Beatty, A. M. *Coord. Chem. Rev.* **2003**, *246*, 131−143.

(5) Molecular Self-Assembly Organic Versus Inorganic Approaches. In *Structure and Bonding*; Fujita, M., Ed.; Springer-Verlag: Berlin, 2000; Vol. 96.

(6) *Crystal Engineering: The Design and Applications of Functional Solids*; Seddon, K. R., Zaworotko, M. J., Eds.; NATO ASI series; Kluwer Academic: Dordrecht, The Netherlands, 1998.

(7) *Crystal Engineering: from Molecules and Crystals of Materials*; Braga, D.; Grepioni, F.; Orpen, A. G., Eds.; NATO ASI series; Kluwer Academic: Dordrecht, The Netherlands, 1999.

(8) Blake, A. J.; Champness, N. R.; Hubberstey, P.; Li, W.-S.; Withersby, M. A.; Schroder, M. *Coord. Chem. Rev.* **1999**, *183*, 117.

(9) Hagrman, P. J.; Hagrman, D.; Zubieta, J. *Angew. Chem., Int. Ed.* **1999**, *38*, 2638−2684.

(10) Batten, S. R.; Robson, R. *Angew. Chem., Int. Ed.* **1998**, *37*, 1460−1494.

(11) Leninger, S.; Olenyuk, B.; Stang, P. J. *Chem. Rev.* **2000**, *100*, 853−908.

(12) Yaghi, O. M.; Li, H.; Davis, C.; Richardson, D.; Groy, T. L. *Acc. Chem. Res.* **1998**, *31*, 474.

(13) Moulton, B.; Zaworotko, M. J. *Curr. Opin. Solid State Mater. Sci.* **2002**, *6*, 117−123.

(14) Recent interesting article for assessment of functionality of coordination polymers: Janiak, C. *J. Chem. Soc., Dalton Trans.* **2003**, 2781−2804.

(15) Benkstein, K. D.; Hupp, J. T.; Stern, C. L. *Angew. Chem., Int. Ed.* **2000**, *39*, 2891−2893.

(16) Wu, Q.; Hook, A.; Wang, S. *Angew. Chem., Int. Ed.* **2000**, *39*, 3933−3935.

(17) Matsuda, K.; Takayama, K.; Irie, M. *Chem. Commun.* **2001**, 363−364.

(18) Slone, R. V.; Hupp, J. T.; Stem, C. L.; Albrecht-Schmitt, T. E. *Inorg. Chem.* **1996**, *35*, 4096−4097.

(19) Slone, R. V.; Benkstein, K. D.; Belanger, S.; Hupp, J. T.; Guzei, I. A.; Rheingold, A. L. *Coord. Chem. Rev.* **1998**, *171*, 221−248.

(20) Belanger, S.; Hupp, J. T.; Stern, C. L.; Slone, R. V.; Wastone, D. F.; Carrel, T. G. *J. Am. Chem. Soc.* **1999**, *121*, 557−563.

(21) Dinolfo, P. H.; Hupp, J. T. *Chem. Mater.* **2001**, *13*, 3113−3125.

(22) Miller, J. S.; Epstein, A. J. *Angew. Chem., Int. Ed. Engl.* **1994**, *33*, 385.

(23) McOuillan, F. S.; Berridge, T. E.; Chen, H.; Hamor, T. A.; Jones, C. J. *Inorg. Chem.* **1998**, *37*, 4959−4970.

(24) Matouzenko, G. S.; Molnar, G.; Brefuel, N.; Perrin, M.; Bousseksou, A.; Borshch, S. A. *Chem. Mater.* **2003**, *15*, 550−556.

(25) Halder, G. J.; Kepert, C. J.; Moubaraki, B.; Murray, K. S.; Cashion, J. D. *Science* **2002**, *298*, 1762−1765.

(26) Chantean, S. H.; Tour, J. M. *Tetrahedron Lett.* **2001**, *42*, 3057−3060.

(27) Dirk, S. M.; Pric, D. W., Jr.; Chantean, S.; Kosynkin, P. V.; Tour, J. M. *Tetrahedron* **2001**, *57*, 5109−5121.

(28) Tour, J. M. *Acc. Chem. Res.* **2000**, *33*, 791−804.

(29) Zaman, M. B.; Tomura, M.; Yamashita, Y. *Org. Lett.* **2000**, *2*, 273−275.

(30) Zaman, M. B.; Smith, M. D.; Ciurtin, D. M.; zur Loye, H.-C. *Inorg. Chem.* **2001**, *40*, 4895−4903.

(31) Dong, Y.-B.; Layland, R. C.; Smith, M. D.; Pschirer, N. G.; Bunz, U. H. F.; zur Loye, H.-C. *Inorg. Chem.* **1999**, *38*, 3056−3060.

(32) Dong, Y.-B.; Layland, R. C.; Pschirer, N. G.; Smith, M. D.; Bunz, U. H. F.; zur Loye, H.-C. *Chem. Mater.* **1999**, *11*, 1413−1415.

(33) Zaman, M. B.; Smith, M. D.; zur Loye, H.-C. *Chem. Mater.* **2001**, *13*, 3534−3541.

(34) Sun, S.-S.; Lees, A. J. *Inorg. Chem.* **1999**, *38*, 4181−4182 and references therein.

(35) For synthesis of 1,4-*bis*[(3-pyridyl)ethynyl]benzene (**L1**), see: Grumt, U.-W.; Brickner, E.; Klemn, E.; Egbe, D. A. M.; Heis, B. *J. Phys. Org. Chem.* **2000**, *13*, 112−126.

(36) Zaworotko, M. J. *Chem. Commun.* **2001**, 1−9.

(37) Kraft, A.; Grimsdale, C. A.; Holmes, B. A. *Angew. Chem., Int. Ed.* **1998**, *37*, 402−406.

(38) Power, K. N.; Hennigar, T. L.; Zaworotko, M. J. *New J. Chem.* **1998**, 177−181.

(39) Choi, H. J.; Suh, M. P. *J. Am. Chem. Soc.* **1998**, *120*, 10622−10623.

(40) Withersby, M. A.; Blake, A. J.; Champness, N. R.; Cooke, P. A.; Hubberstey, P.; Li, W.-S.; Schroder, M. *Inorg. Chem.* **1999**, *38*, 2259−2266.

(41) Ino, I.; Wu, L. P.; Munakata, M.; Maekawa, M.; Suenaga, Y.; Kuroda-Sowa, T.; Kitamori, Y. *Inorg. Chem.* **2000**, *39*, 2146−2151.

(42) Evans, O. R.; Lin, W. *Inorg. Chem.* **2000**, *39*, 2189−2198.

(43) Dong, Y.-B.; Smith, M. D.; Layland, R. C.; zur Loye, H.-C. *Chem. Mater.* **2000**, *12*, 1156−1161.

(44) Ciurtin, D. M.; Dong, Y.-B.; Smith, M. D.; Barclay, T.; zur Loye, H.-C. *Inorg. Chem.* **2001**, *40*, 2825−2834.

interconnected by a spacer, yielding a wide variety of lengths, linear or nonlinear geometries, and conformationally rigid or nonrigid molecular skeletons.

While it has been suggested by Batten and Robson that longer ligands will favor the formation of interpenetrating over noninterpenetrating grid structures,[10] it appears that the incorporation of spacer benzene rings [e.g., 1,4-bis(4′-pyridyl)biphenly] can inhibit interpenetrating and enable the formation of large square grids with infinite channels.[45] The long, rigid ligands of different lengths and dimensions can control the size and shape of the macrocyclic polymers, as well as the functionality of the framework structure. Very recently, we explored two new long, rigid *N,N′*-bipyridine-based ligands, 9,9-diethyl-2,7-bis(4-pyridylethynyl)fluorene and chiral 9,9-bis[(*S*)-2-methylbutyl]-2,7-bis(4-pyridyl-ethynyl)fluorine, and their role in the formation of non-interpenetrating square-grid polymers containing chiral and nonchiral chemical environments in the large channels.[46] In this work, we have chosen to employ two long, rigid bipyridyl-based ligands, 1,4-bis[(3-pyridyl)ethynyl]benzene (**L1**) and 1,4-bis[(4-pyridyl)ethynyl]benzene (**L2**), in reaction with Co(NO$_3$)$_2$·6H$_2$O, Cd(NO$_3$)$_2$·4H$_2$O, Cu(NO$_3$)$_2$·3H$_2$O, and Cu(hfac)$_2$·H$_2$O (hfac = hexafluoroacetylacetonate), to direct the formation of organic–inorganic coordination polymers with or without interpenetration. In a preliminary communication, we have reported the long, rigid organic ligand, **L2**, and its reaction with copper nitrate, constructing two dissimilar motifs that coexist in the same structure.[47] Such a novel structural motif consisting of stacks of infinite ladders interpenetrated by the bundles of infinite chains is a rare and attractive one. In this paper, we report our efforts in the design and synthesis of long, rigid organic ligands that self-assemble into diverse organic–inorganic polymeric networks consisting of one-, two-, or three-dimensional structures. Four crystalline coordination polymers were obtained from the **L1** ligand, [Cd(C$_{20}$H$_{12}$N$_2$)$_{0.5}$(NO$_3$)(CH$_3$OH)]$_n$ (**1**), [{Cu(C$_{20}$H$_{12}$N$_2$)(NO$_3$)$_2$(CH$_3$OH)}·CH$_3$OH]$_n$ (**2**), [Cu-(C$_{20}$H$_{12}$N$_2$)(NO$_3$)]$_n$ (**3**), and [Cu(C$_{20}$H$_{12}$N$_2$)(hfac)$_2$]$_n$ [hfac = bis(hexafluoroacetylacetonato)] (**4**), which form inter-penetrating 2D and 3D cross–zigzag chains, metallocyclic chain structures. Moreover, the dinuclear coordination complex Co(C$_{20}$H$_{12}$N$_2$)$_2$(NO$_3$)$_2$(H$_2$O)$_2$ (**5**) was also formed from the **L1** ligand, in which strong hydrogen-bonded interactions created a polymeric infinite chain. Five other distinct crystalline coordination polymers were synthesized from the **L2** ligand. These are [Co(C$_{20}$H$_{12}$N$_2$)$_{1.5}$(NO$_3$)$_2$]$_n$ (**6**), an interpenetrating ladder network with a polycatenane architecture; [Cd(C$_{20}$H$_{12}$N$_2$)$_2$(NO$_3$)$_2$]$_n$ (**7**), a noninterpenetrating square-grid network with dimensions of (20 × 20 Å^2); [Cu(C$_{20}$H$_{12}$N$_2$)(hfac)$_2$]$_n$ (**8**) [hfac = bis(hexafluoroacetyl-acetonato)], a network of one-dimensional linear chains; [Cu(C$_{20}$H$_{12}$N$_2$)(EtOH)(NO$_3$)$_2$] [Cu(C$_{20}$H$_{12}$N$_2$)$_{1.5}$(NO$_3$)$_2$]·2EtOH (**9**), two different one-dimensional structural motifs in a

single crystal containing ethanol; and [Cu(C$_{20}$H$_{12}$N$_2$)(MeOH)-(NO$_3$)$_2$] [Cu(C$_{20}$H$_{12}$N$_2$)$_{1.5}$(NO$_3$)$_2$]·2MeOH (**10**), two different one-dimensional structural motifs in a single crystal containing methanol. Both the novel structures **9** and **10** stack into infinite ladders of composition [Cu(C$_{20}$H$_{12}$N$_2$)$_{1.5}$(NO$_3$)$_2$] and are interpenetrated by infinite chains of composition [Cu(C$_{20}$H$_{12}$N$_2$)(solvent)(NO$_3$)$_2$]. The structures **9** and **10** were reported in our preliminary communication and are not described here.

Experimental Section

Materials and Methods. The ligands 1,4-bis[(3-pyridyl)ethynyl]-benzene (**L1**)[35] and 1,4-bis[(4-pyridyl)ethynyl]benzene (**L2**)[48] were prepared according to a literature method.[49] Single crystals suitable for X-ray analysis were obtained for **L2** by recrystallization from benzene.[50] The commercially available metal salts, Cd(NO$_3$)$_2$·4H$_2$O, Co(NO$_3$)$_2$·6H$_2$O (both from Aldrich, 98%), Cu(NO$_3$)$_2$·3H$_2$O (Alfa Aesar, Technical Grade), and Cu(hfac)$_2$·H$_2$O (Aldrich, 99%), were used without further purification. IR spectra were recorded on a Nicolet 740 FTIR and Varian 450 FTIR spectrometers as KBr pellets in the range 4000−400 cm^{-1}. Thermogravimetric analyses were carried out on commercial TA SDT 2960 simultaneous DTA-TGA instrument under flowing helium and TA Instruments TGA 2050 under flowing nitrogen. Compounds **1**−**10** were heated from 50 to 800 °C at a rate of 10 °C/min.

X-ray Structure Determinations. X-ray diffraction experiments were performed on single crystals, or chips cut from there, taken from their respective mother liquors and cooled immediately to −100 °C. A Siemens SMART CCD diffractometer equipped with graphite-monochromatized Mo Kα radiation (λ = 0.71070 Å) (for compounds **1**− **5**) and a Bruker SMART APEX CCD-based diffractometer (Mo Kα radiation, λ = 0.71073 Å) (for compounds **6**−**8**) were used to collect the diffraction data. Preliminary unit cell dimensions were obtained by using 60 or more frame ω scans, 0.3° wide, starting at three different ϕ positions. Complete data sets were collected in the ω scan mode over the 2θ range of 3−58°. Coverage of the unique sets was over 99%. Empirical absorption corrections were performed utilizing the SADABS suite of programs associated with the diffractometer. The final unit cell parameters were obtained by incorporating the entire data set. All structures were solved by direct methods and were refined against F^2 by full-matrix least-squares techniques using the SHELXTL software package.[51,52] Hydrogen atoms were placed in calculated positions and were refined as riding atoms; all nonhydrogen atoms including solvent molecules were refined with anisotropic thermal displace-ment parameters. Crystal data and refinement statistics for com-pounds **1**−**5** and **6**−**8** are given in Tables 1 and 2, respectively.

Synthesis. [Cd(C$_{20}$H$_{12}$N$_2$)$_{0.5}$(NO$_3$)(CH$_3$OH)]$_n$ (1). A colorless solution of Cd(NO$_3$)$_2$·4H$_2$O (30.9 mg, 0.1 mmol) in methanol (5

(45) Biradha, K.; Hongo, Y.; Fujita, M. *Angew. Chem., Int. Ed.* **2000**, *39*, 3943−3845.

(46) Pschirer, N. G.; Ciurtin, D. M.; Smith, M. D.; Bunz, U. H. F.; zur Loye, H.-C. *Angew. Chem., Int. Ed.* **2002**, *41*, 583−585.

(47) Zaman, M. B.; Smith, M. D.; zur Loye, H.-C. *Chem. Commun.* **2001**, 2256−2257.

(48) For synthesis of 1,4-*bis*[(4-pyridyl)ethynyl]benzene (**L2**), see: Lin, J. T.; Sun, S.-S.; Wu, J. J.; Lee, L.; Lin; K.-J.; Huang, Y. F. *Inorg. Chem.* **1995**, *34*, 2323−2333.

(49) Convenient routes for the synthesis of ethynylpyridines see: Rodriguez, J. G.; Martine-Villamil, R.; Cano, F. H.; Fonseca, I. *J. Chem. Soc., Perkin Trans. 1* **1997**, 709−714.

(50) To our knowledge, the structure of ligand **L2** is not known. We first stated the single-crystal X-ray data of ligand **L2** including a recrys-tallization solvent benzene. Crystal data for **L2**: C$_{26}$H$_{18}$N$_2$, *M* = 358.42, monoclinic, space group *P*2$_1$/*n*, *a* = 11.072(1), *b* = 7.364(1), *c* = 11.866(1) Å, β = 94.592(2)°, *V* = 964.3(2) Å^3, *Z* = 2, *T* = 173(2) K, *R$_1$* = 0.0420, *wR$_2$* = 0.1034 for 1703 data with *I* > 2σ (*I*).

(51) Sheldrick, G. M. *Acta Crystallogr., Sect. A* **1990**, *46*, 467; **1993**, *49*, C467.

(52) SMART, SAINT, and SHELX software, Bruker Analytical X-ray System Inc., WI, 1997.

Table 1. Crystallographic Data for **1−5**

	1	**2**	**3**	**4**	**5**
empirical formula	$C_{22}H_{20}CdN_4O_8$	$C_{22}H_{20}CuN_4O_8$	$C_{40}H_{20}CuN_6O_6$	$C_{46}H_{18}CuF_{12}N_2O_4$	$C_{40}H_{28}CoN_6O_8$
mol wt	580.82	513.96	748.19	727.82	779.61
cryst syst	monoclinic	orthorhombic	triclinic	monoclinic	triclinic
a (Å)	7.586(1)	8.589(1)	8.728(1)	18.828(1)	7.493(1)
b (Å)	23.222(1)	15.766(1)	10.018(1)	14.671(1)	8.948(1)
c (Å)	13.572(1)	17.501(1)	11.893(1)	13.427(1)	14.854(1)
α (deg)	90.00	90.00	109.991(1)	90.00	100.427(1)
β (deg)	92.824(1)	90.00	97.109(1)	90.447(1)	97.324(1)
γ (deg)	90.00	90.00	115.542(1)	90.00	110.901(1)
V (Å³)	2388.0(2)	2370.4(4)	851.4(1)	3702.1(3)	894.8(1)
space group	$C2/c$	$P2_12_12_1$	$P\bar{1}$	$C2/c$	$P1$
Z value	4	4	1	4	1
ρ_{calc} (g/cm³)	1.616	1.491	1.459	1.667	1.447
μ (MoKα) (cm⁻¹)	0.0969	0.0976	0.0701	0.0979	0.0544
λ (Å)	0.71070	0.71070	0.71070	0.71070	0.71070
temp (°K)	173(2)	173(2)	173(2)	173(2)	173(2)
residuals:[a] R; R_w	0.056; 0.132	0.024; 0.060	0.032; 0.082	0.049; 0.145	0.027; 0.0711
GOF	1.215	1.022	1.037	1.033	1.048

[a] $R1 = \sum||F_o| - |F_c||/\sum|F_o|$. $wR2 = \{\sum[w(F_o^2 - F_c^2)^2]/\sum[w(F_o^2)^2]\}^{1/2}$; GOF $= \{\sum[w(F_o^2 - F_c^2)^2]/(n - p)\}^{1/2}$ (n = no. refl; p = no. refined parameters). $w = 1/[\sigma^2(F_o^2) + (aP)^2 + bP]$, where P is $[2F_c^2 + \max(F_o^2, 0)]/3$.

Table 2. Crystallographic Data for **6−8**

	6	**7**	**8**
empirical formula	$C_{30}H_{18}CoN_5O_6$	$C_{40}H_{24}CdN_6O_6$	$C_{30}H_{14}CuF_{12}N_2O_4$
mol wt	603.42	797.05	757.97
cryst syst	triclinic	monoclinic	monoclinic
a (Å)	14.172(1)	11.371(1)	10.613(1)
b (Å)	15.795(1)	20.311(2)	20.562(2)
c (Å)	18.072(1)	15.240(2)	14.701(2)
α (deg)	115.380(1)	90.00	90.00
β (deg)	101.319(1)	100.201(2)	98.637(1)
γ (deg)	93.427(2)	90.00	90.00
V (Å³)	3535.6(4)	3464.1(6)	3172.4(4)
space group	$P\bar{1}$	$I2/a$	$I2/a$
Z value	4	4	4
ρ_{calc} (g/cm³)	1.134	1.528	1.587
μ (MoKα) (cm⁻¹)	0.0527	0.0689	0.0797
λ (Å)	0.71073	0.71073	0.71073
temp (°K)	173(2)	293(2)	173(2)
residuals:[a] R; R_w	0.060; 0.123	0.040; 0.104	0.035; 0.096
GOF	0.993	1.063	1.034

[a] $R1 = \sum||F_o| - |F_c||/\sum|F_o|$. $wR2 = \{\sum[w(F_o^2 - F_c^2)^2]/\sum[w(F_o^2)^2]\}^{1/2}$; GOF $= \{\sum[w(F_o^2 - F_c^2)^2]/(n - p)\}^{1/2}$ (n = no. refl; p = no. refined parameters). $w = 1/[\sigma^2(F_o^2) + (aP)^2 + bP]$, where P is $[2F_c^2 + \max(F_o^2, 0)]/3$.

mL) was carefully layered onto a solution of **L1** (28.0 mg, 0.1 mmol) in methylene chloride (10 mL). Diffusion between the two phases over a period of 2 days produced a multifaceted white crystal in 92% yield on the basis of cadmium nitrate. IR (KBr, cm⁻¹): 1756 (w), 1688 (s), 1536 (m), 1444 (w), 1416 (s), 1333 (s), 1244 (s), 1090 (s), 1055 (m), 842 (s), 787 (s), 732 (w).

[{Cu(C$_{20}$H$_{12}$N$_2$)}(NO$_3$)$_2$(CH$_3$OH)]·CH$_3$OH]$_n$ (2), [Cu(C$_{20}$H$_{12}$N$_2$)-(NO$_3$)]$_n$ (3). A methanol solution of Cu(NO$_3$)$_2$·3H$_2$O (24.2 mg, 0.1 mmol) was slowly added to a methylene chloride (12 mL) solution of **L1** (28.1 mg, 0.1 mmol). After a day, the bluish solution was evaporated (at room temperature) over a period of 3 days to half the initial volume. After 2 more days, bluish-green crystals, and a few soft greenish-blue crystals, grew at the bottom of the test tube in 62% yield on the basis of copper nitrate. IR (KBr, cm⁻¹): 1699 (s), 1589 (w), 1467 (m), 1444 (s), 1380 (s), 1300 (s), 1235 (m), 1060 (m), 1015 (m), 950 (w), 880 (w). **2** and **3** form simultaneously in the same batch of crystals and, consequently, the yield and IR data apply to the mixture of **2** and **3**. We observed that the bluish-green crystal **2** is a major product in the reaction mixture and is unstable at room temperature.

[Cu(C$_{20}$H$_{12}$N$_2$)(hfac)$_2$]$_n$ (4). A methanol solution of **L1** (0.1 mmol) was slowly diffused over a methylene chloride solution of Cu(hfac)$_2$·H$_2$O (0.1 mmol, 5 mL) through a layer of an ethanol/hexane (2:1) mixture. After a day, bright green crystals formed in 88% yield on the basis of copper(II) hexafluoroacetylacetonate hydrate. IR (KBr, cm⁻¹): 1782 (w), 1690 (s), 1640 (s), 1560 (m), 1480 (s), 1454 (w), 1400 (s), 1330 (s), 1255 (s), 1080 (s), 1065 (m), 950 (s), 810 (s), 795 (m), 750 (m), 735 (m).

Co(C$_{20}$H$_{12}$N$_2$)$_2$(NO$_3$)$_2$(H$_2$O)$_2$ (5). Compound **5** was synthesized in a similar way to **1**, except that Co(NO$_3$)$_2$·6H$_2$O was replaced by Cd(NO$_3$)$_2$·4H$_2$O. In 7 days, bright yellowish-red crystals were obtained in 48% yield on the basis of cobalt nitrate. IR (KBr, cm⁻¹): 1630 (s), 1583 (w), 1465 (m), 1476 (s), 1355 (s), 1320 (s), 1235 (m), 1065 (m), 1005 (m), 985 (w), 850 (w).

[Co(C$_{20}$H$_{12}$N$_2$)$_{1.5}$(NO$_3$)$_2$]$_n$ (6). A solution of Co(NO$_3$)$_2$·6H$_2$O (0.1 mmol) in an ethanol (15 mL) mixture was allowed to diffuse slowly into an ethanol (10 mL) solution of **L2** (0.1 mmol). Immediately, an orange precipitate formed at the interface of two layers. Reddish-orange crystals formed after overnight slow evaporation in this mixture. The yield was 42% on the basis of cobalt nitrate hexahydrate. IR (KBr, cm⁻¹): 1661 (w), 1613 (w), 1588 (m), 1468 (m), 1464 (m), 1362 (s), 1318 (m), 1230 (m), 1076 (s), 1016 (s), 910 (w).

[Cd(C$_{20}$H$_{12}$N$_2$)$_2$(NO$_3$)$_2$]$_n$ (7). Compound **7** was synthesized in a similar way to that used for **6**, except that Co(NO$_3$)$_2$·6H$_2$O was replaced by Cd(NO$_3$)$_2$·4H$_2$O. Pinkish-white crystals were obtained in 25% yield on the basis of cadmium nitrate. IR (KBr, cm⁻¹): 1778 (w), 1665 (m), 1555 (m), 1476 (w), 1456 (m), 1365 (s), 1310 (s), 1266 (s), 1058 (m), 1022 (s), 947 (w).

[Cu(C$_{20}$H$_{12}$N$_2$)(hfac)$_2$]$_n$ (8). Compound **8** was synthesized using a procedure similar to that used for **4**. Deep green crystals were obtained in 94% yield on the basis of copper(II) hexafluoroacetylacetonate hydrate. IR (KBr, cm⁻¹): 1776 (w), 1688 (m), 1648 (s), 1571 (s), 1487 (s), 1466 (w), 1428 (m), 1336 (s), 1262 (s), 1078 (s), 1045 (m), 928 (s), 811 (s), 775 (m), 732 (m), 702 (s).

Results and Discussion

Synthesis. Ten new coordination polymers were synthesized by solution reactions between the two ligands **L1** (1,4-bis[(3-pyridyl)ethynyl]benzene) and **L2** (1,4-bis[(4-pyridyl)-ethynyl]benzene) with the metal salts M(NO$_3$)$_2$·xH$_2$O; M = Cd(II), Co(II), and Cu(II); x = 3−6 and Cu(hfac)$_2$·H$_2$O [hfac

= bis(hexafluoroacetylacetonato)]. Single crystals of compounds **1**−**5**, **8**, and **10** were all obtained from the same methanol/methylene chloride solvent system, although their respective preparation routes differed slightly. When a solution of **L1** in methylene chloride was treated with $M(NO_3)_2 \cdot xH_2O$ in methanol, using a metal-to-ligand ratio of 1:1, compounds **1**−**5** were obtained as crystalline polymeric compounds displaying two principal architectures: layers (**3**, **5**) and chains (**1**, **2**, **4**, **5**). Slow diffusion of $Cu(NO_3)_2 \cdot 3H_2O$ in methanol into a methylene chloride solution of **L1** afforded a mixture of two crystalline coordination polymers (**2** and **3**) within 1 week. When crystals of compound **2** were removed from the mother liquor, they quickly lost solvent, became opaque and brittle, and eventually collapsed into a bluish powder. However, when coated with a viscous oil, they were sufficiently stable for crystallographic analysis. We were unable to grow high-quality single crystals of **5** by an analogous slow diffusion of $Co(NO_3)_2 \cdot 6H_2O$ in methanol into a methylene chloride solution of **L1**. However, we were able to grow large reddish-orange crystals of **6** by overnight slow evaporation of an ethanol-diffused reaction mixture in a test tube. The interpenetrating polymeric square-grid architecture of compound **7** was obtained from an ethanol system as well. Deep blue-green crystals of **9** and **10** were obtained by allowing an ethanol and methanol solution of $Cu(NO_3)_2 \cdot 3H_2O$, respectively, to diffuse into a methylene chloride solution of **L2**. Compounds **1**, **3**, **9**, and **10** all decompose when removed from the mother liquor, though not as quickly as **2**, presumably because of loss of incorporated solvent from the framework. Compounds **1**−**10** are insoluble in both water and common organic solvents.

Zigzag Chain Structures. Three polymeric zigzag chain motifs are exemplified by the polymeric structures **1**, **2**, and **4**, produced by reaction of cadmium nitrate, copper nitrate, and copper bis(hexafluoroacetylacetonato), respectively, with ligand **L1**. The fourth zigzag chain motif is characterized by the infinite hydrogen-bonded system of the dinuclear complex of **5**, produced by reaction of cobalt nitrate with ligand **L1**. Zigzag chains containing other metals, such as Cd, Cu, Ag, and Mn, have been reported previously.[33,53−57] Compound **5** is the rare example of a hydrogen-bonded zigzag chain containing cobalt nitrate. The polymeric single crystals of cobalt nitrate and ligand **L1** are, in general, not obtained by employing a wide variety of standard synthetic methods encompassing single and mixed solvent systems.

The immediate coordination environment around the cadmium center in compound **1** is shown in Figure 1. The
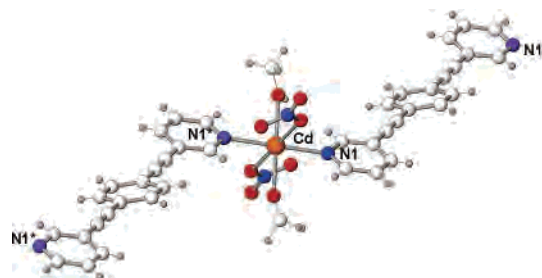

Figure 1. Cadmium coordination environment with major atom numbering scheme in **1**. Displacement ellipsoids shown at the 50% probability level. Disordered atoms from coordinated methanol are removed. Asterisks denote symmetry equivalent atoms.

Cd(II) ions lie in a pseudo-octahedral six-coordinated center, consisting of two oxygen donors from disordered nitrate anions, two oxygen donors from disordered methanol molecules, and two pyridyl nitrogen atoms from two **L1** ligands. Crystallographically equivalent bond distances around the Cd center are typical of other cadmium-based coordination polymers containing nitrogen donor ligands: N−Cd = 2.310 Å for **L1** and Cd−O = 2.302 and 2.346 Å for nitrate and methanol, respectively, consistent with corresponding bond lengths found in $[Cd(NO_3)_2(1,2\text{-bis(4-pyridyl)ethene/ethyne})_{1.5}]_n$,[31] $[Cd(NO_3)_2(4,4'\text{-bipy})_2 \cdot 2C_6H_4Br_2]_n$,[58] and $[Cd(NO_3)_2(dpb)_{1.5}]_n$.[59] The ligands are coordinated in a trans fashion, with N(1)−Cd−N(2)* = 180.0°. The pyridyl rings lie in a plane and are rotated 20.6° with respect to the spacer benzene ring. This linear coordination geometry, in combination with the **L1** ligand three positional nitrogen atoms, results in a zigzag chain motif. The view of these zigzag chains along the diagonal line of the *ac*-plane is shown in Figure 2a. The interlayer distance between cadmium atoms is 7.586 Å, and two-dimensional corrugated sheets type architecture can be viewed in Figure 2b.

The structure of compound **2**, emphasizing the coordination environment around the copper, is shown in Figure 3. Each copper(II) center lies in a pseudo-square-pyramidal coordination environment consisting of two bidentate nitrates, one **L1** ligand in the basal plane and the other **L1** ligand in a trans position, and one methanol solvent. The axial positions are occupied by pyridyl nitrogen donors from the ligand **L1** (N(1)−Cu = 2.022(1) Å), and the equatorial positions are occupied by trans oxygen atoms from nitrate anions (Cu−O(1) = 2.006(3) Å, Cu−O(4) = 1.993(4) Å) and oxygen atom from a methanol molecule (Cu−O(1A) = 2.246(4) Å). The bond distances between the Cu(II) and the two nitrate oxygens and one oxygen belonging to the methanol molecule are shorter than those found in related compounds.[33,55,60−62] In a manner similar to compound **1**, in **2** the two pyridyl nitrogen atoms of the two **L1** ligands are

(53) Bakalbassis, E. G.; Korabik, M.; Michailides, A.; Mrozinski, J.; Raptopoulou, C.; Skoulika, S.; Terzis, A.; Tsaousis, D. *J. Chem. Soc., Dalton Trans.* **2000**, 850−857.

(54) Graham, P. M.; Pike, R. D.; Sabat, M.; Bailey, R. D.; Pennington, W. M. *Inorg. Chem.* **2000**, *39*, 5121−5132.

(55) Carlucci, L.; Ciani, G.; Proserpio, D. M.; Rizzato, S. *J. Chem. Soc., Dalton Trans.* **2000**, 3821−3827.

(56) Su, C.-Y.; Goforth, A. M.; Smith, M. D.; zur Loye, H.-C. *Chem. Commun.* **2004**, 2158−2159 and references cited therein.

(57) Withersby, M. A.; Blake, A. J.; Champness, N. R.; Cooke, P. A.; Hubbersty, P.; Scroder, M. *J. Am. Chem. Soc.* **2000**, *122*, 4044−4046.

(58) Fujita, M.; Kwon, Y. J.; Washizu, S.; Ogura, K. *J. Am. Chem. Soc.* **1994**, *116*, 1151−1152.

(59) Fujita, M.; Kwon, Y. J.; Sasaki, O.; Yamaguchi, K.; Ogura, K. *J. Am. Chem. Soc.* **1995**, *117*, 7287−7288.

(60) Carlucci, L.; Ciani, G.; Proserpio, D. M. *Chem. Commun.* **1999**, 449−450.

(61) Batten, S. R.; Harris, A. R.; Jensen, P.; Murray, K. S.; Ziebell, A. *J. Chem. Soc., Dalton Trans.* **2000**, 3829−3835.

(62) Tong, M.-L.; Chen, X.-M.; Yu, X.-L.; Mak, T. C. W. *J. Chem. Soc., Dalton Trans.* **1998**, 5−6.
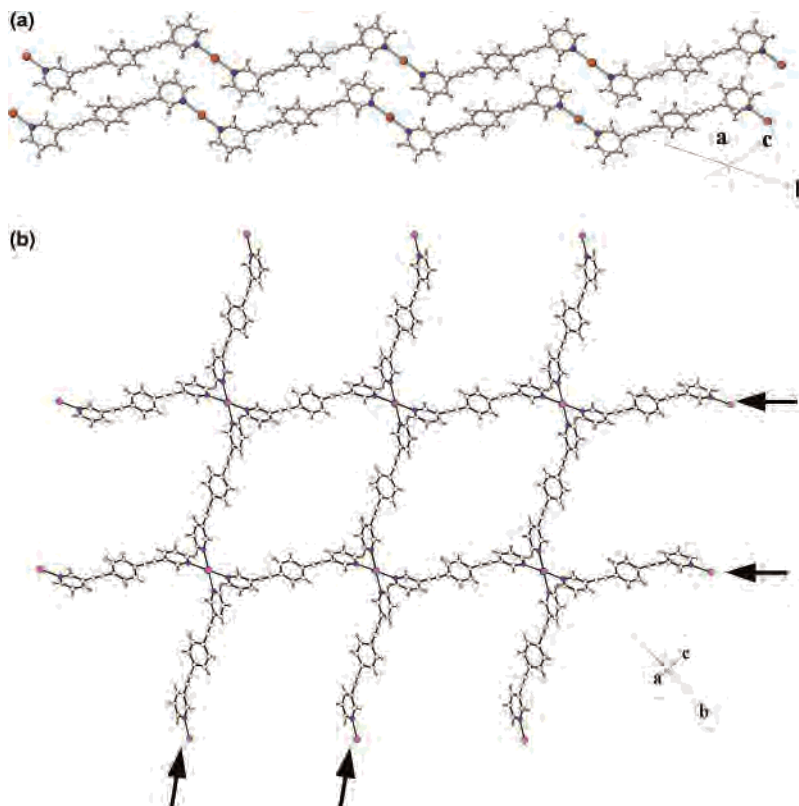
Figure 2. View of zigzag chain architecture in **1** along the diagonal line of the *ac*-plane (a) one-dimensional observation (b) two-dimensional view between two adjacent chains. Coordinated nitrates and methanol are omitted for clarity.
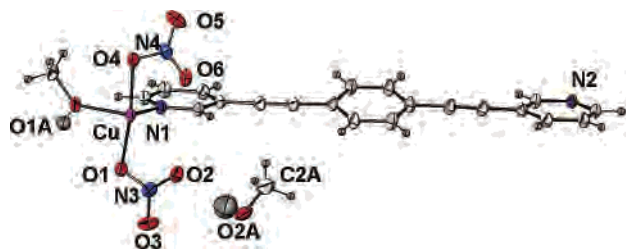

Figure 3. The asymmetric unit of compound **2** including the methanol solvent (50% probability ellipsoids).

coordinated to the metal center in a trans fashion (N(1)−Cd−N(2)* = 180.0°) and form a 1D zigzag polymeric chain (Figure 4a). In **2**, however, the pair of associated 1D zigzag chains is arranged in layers parallel to the crystallographic *bc* plane. Figure 4b shows the linking of two crystallographically equivalent chains into the dual strands that make up compound **2**. Moreover, the chain pairs interact side-by-side via the guest methanol molecules by hydrogen bonding between chain pairs (O1A···O2A = 2.625() Å; O2···O2A = 2.806() Å; ∠(O1A···O2A···O2) = 125(5)°). The pairs of associated chains are rotated by 90° followed by stacking of these layers of dual chains along [001] that comprises the 3D crystal structure. Figure 5 depicts a view perpendicular to the stacking direction [001], illustrating the 3D crisscrossing of chains. The structural motifs of **1** and **2** reported herein are, to the best of our knowledge, unprecedented and represent new polymeric frameworks generated from the long linear spacer ligand **L1**.

The polymeric framework of compound **4** crystallizes in the monoclinic space group *C*2/*c* and is analogous to that of

our previously reported compounds on the basis of bis-(hexafluoroacetylacetonato)M (M = Cu, Mn, Zn)[63] metal salts. The immediate coordination environment about the metal center (Figure 6) is 4 + 2 pseudooctahedral with a trans fashion of the pyridine rings (N1−Cu−N1* = 180.0°), where the three positional orientations of pyridyl nitrogen atoms induce the formation of a 1D zigzag polymeric chain. The bond lengths [Cu−N = 2.003(2) Å, Cu−O1 = 2.000(2) Å, and Cu−O2 = 2.312(2) Å] in compound **4** are slightly shorter than those of similar polymeric motifs reported previously.[64,65] Interestingly, there are two distinct 1D nets in **4** that lie along the directions [212] and [221] and stack together in an ...ABAB... fashion down the crystallographic *c*-axis, such that a pair of zigzag chain networks stack upon one another and generate a 2D layer architecture. The closest Cu···Cu contact between two adjacent chains is 9.944 Å. The manner in which these undulating chains stack upon one another is given in Figure 7. In the absence of guest inclusion, such a 2D architecture that formed from bis-(hexafluoroacetylacetonato) metal salts has been only rarely reported.[66]

The immediate coordination arrangement around the cobalt center in compound **5** is shown in Figure 8. The Co(II) ions lie in an octahedral environment, consisting of two pyridyl

(63) Zaman, M. B.; Udachin, K. A.; Ripmeester, J. A. *CrystEngComm* **2002**, *4* (103), 613−617.
(64) Ellis, W. W.; Schmitz, M.; Arif, A. M.; Stang, P. J. *Inorg. Chem.* **2000**, *39*, 2547−2557.
(65) Matsuda, K.; Takayama, K.; Irie, M. *Chem. Commun.* **2001**, 363−364.
(66) Tabellion, F. M.; Seidel, S. R.; Arif, A. M.; Stang, P. J. *J. Am. Chem. Soc.* **2001**, *123*, 11982−11990.
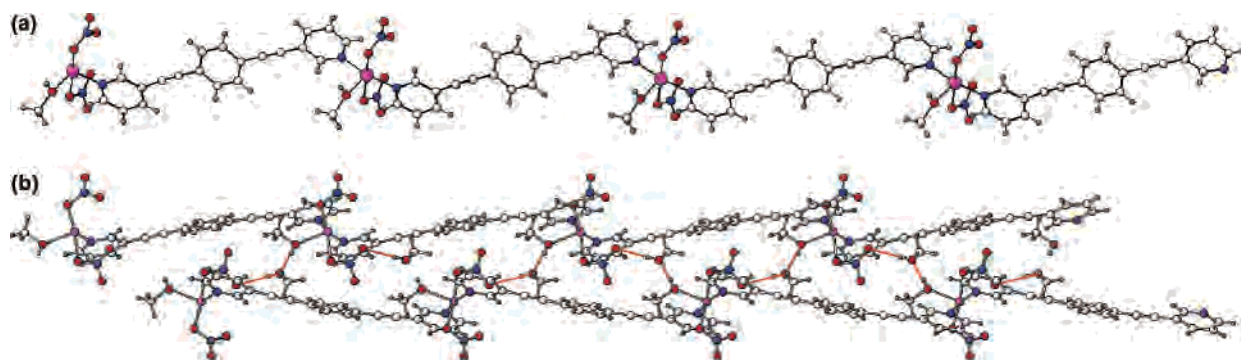
Figure 4. (a) View of the one-dimensional zigzag chain architecture of **2**. (b) The chains are hydrogen-bonding interactions of coordinated methanol and nitrate via methanol solvent. The view is shown parallel to the crystallographic *bc* plane.
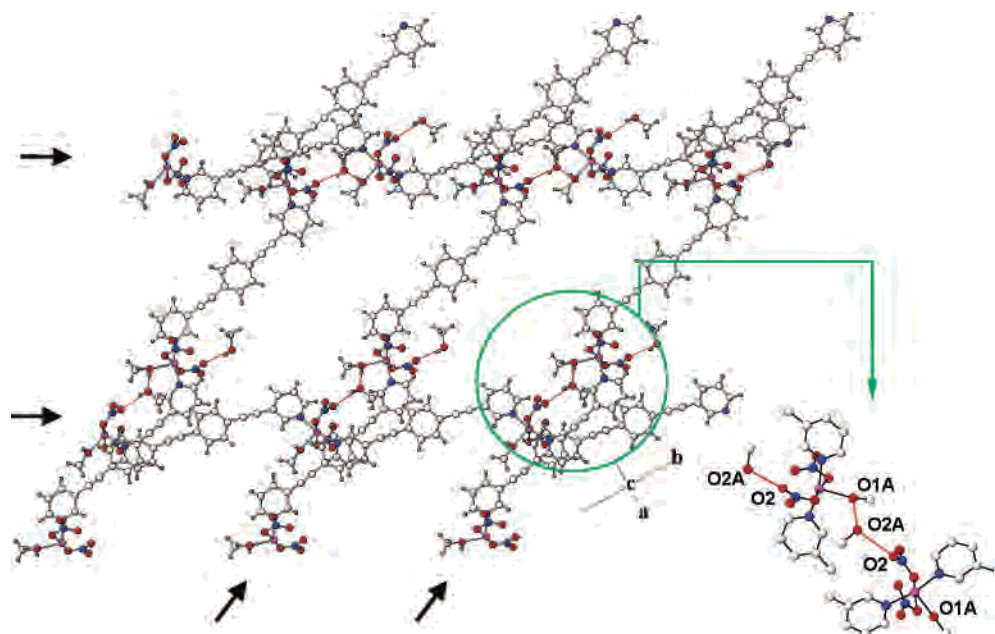

Figure 5. View down the stacking direction ([001]) of two crisscrossing layers of zigzag chains in **2**. Interchain hydrogen bonds are shown as red lines. Hydrogen atoms are omitted in the wider presentation.
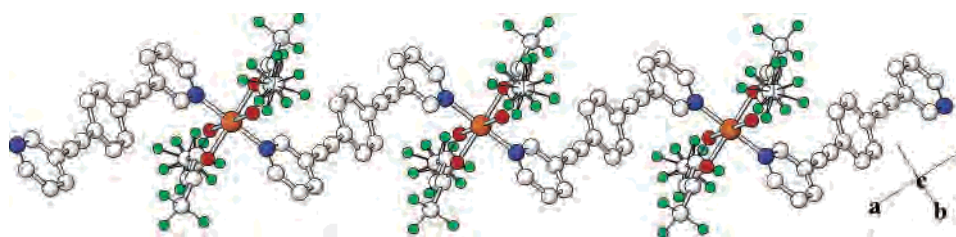

Figure 6. View of the one-dimensional zigzag chain of **4**.

nitrogen atoms from two **L1** ligands, two oxygen atoms from two nitrate anions, and two oxygen atoms from two water molecules. The Co–N and Co–O bond lengths [Co–N(1) = 2.100(1) Å, Co–N(3) = 2.169(1) Å, Co–O = 2.060(1)–2.138(1) Å] are close to the corresponding bond lengths generally found in the literature.[33,44,67] The **L1** ligands are coordinated in a trans fashion, with N(1)–Co–N(3) = 179.7(1)°. The pyridyl rings in **L1** are rotated by almost 90° relative to one another, similar to what was previously

observed in cobalt–3,3′-bipyridine compounds.[67] A twisting trend of the pyridyl rings and three-fold positional orientation of nitrogen atoms of the **L1** ligand is thrown into disarray by the coordination of pyridyl nitrogen atoms to another Co center to form a polymeric network. Thus, a dinuclear coordination complex of **5** is formed with strong hydrogen-bonding interactions between the coordinated water molecules and the pyridyl nitrogen atoms of the dinuclear complexes, resulting in an infinite zigzag chain motif. Interestingly, the adjacent dinuclear complexes are in turn hydrogen-bonded to the coordinated water molecules and the

(67) Dong, Y.-B.; Smith, M. D.; zur Loye, H.-C. *J. Solid State Chem.* **2000**, *155*, 143153.
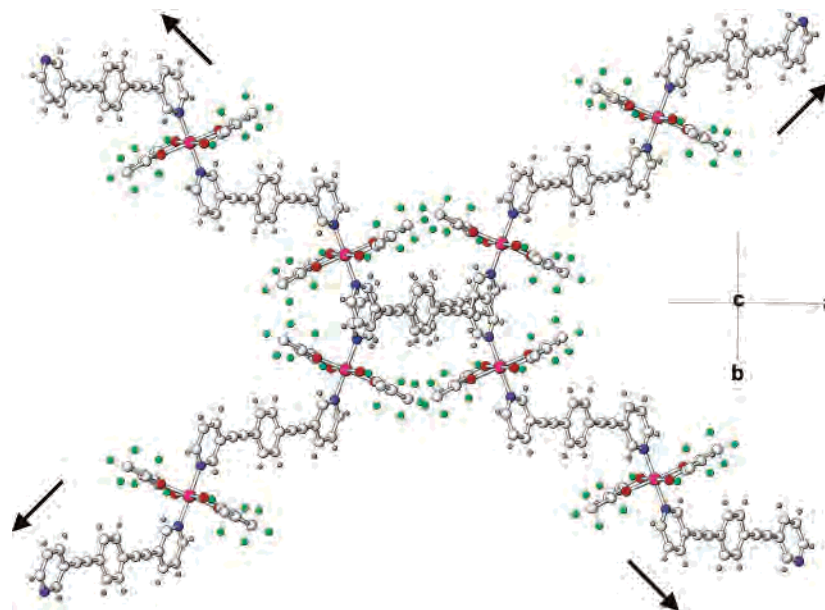
Figure 7. Overlapping of ligands **L1** in **4** and their two-dimensional cross-linking is shown; the view is down the *c*-axis.
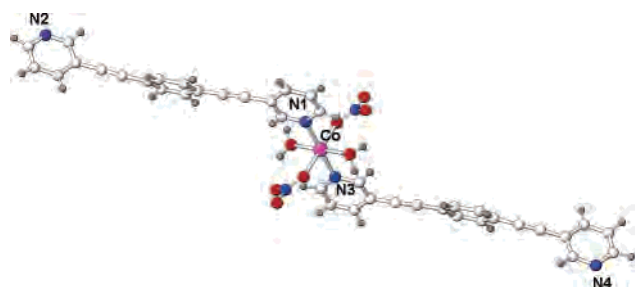

Figure 8. The local coordination environment around the Co atom in **5** is shown with the selected atomic numbering scheme. Ellipsoids are shown at 50% probability level.

unbound pyridyl nitrogen atoms (O2−H21W···N4; d(H···N) = 1.840(1) Å, ∠(O−H···N) = 173.66(1)°; O1−H12W···N2; d(H···N) = 1.756(1) Å, ∠(O−H···N) = 174.32(1)°) thereby completing the hydrogen-bonded metallocyclic architectures. A schematic of this novel metallocyclic chain architecture is shown in Figure 9a. In addition, two adjacent infinite zigzag chains (or macrocyclic chains) are again hydrogen-bonded to the coordinated water molecules and the nitrate anions (O1−H11W···O5; d(H···O) = 2.270(1) Å, ∠(O−H···O) = 139.36(1)°; O2−H22W···O8; d(H···O) = 2.548(1) Å, ∠(O−H···O) = 106.17(1)°), as well as between the nitrate ions (d(O4···O7) = 2.922 Å) thereby forming Co−(H$_2$O)$_2$···(NO$_3$)$_2$−Co and Co−(NO$_3$)$_2$···(NO$_3$)$_2$−Co bridges along the crystallographic *a* axis, with a Co···Co distance of 7.493 Å (Figure 9b). Compound **5** thus assembles into a two-dimensional hydrogen-bonded infinite structure.

The {CoN$_2$O$_4$} coordination sphere in **5** is unusual in hydrogen-bonding frameworks. The less sterically crowded six-coordinate environment may primarily be responsible for the slightly shorter Co−N and Co−O bond distances observed. Such octahedral geometries have also been found in [Co(NO$_3$)$_2$(H$_2$O)$_2$(1,2-bis(3-pyridyl)ethene)·(H$_2$O)]$_n$,[33] where two pyridine rings are twisted to 70°, and coordinated to the Co(II) atoms to form infinite linear chains. In the case

of **5**, the unusual macrocyclic-chain motif is generated by the location of the nitrogen atoms in the three-position on the pyridine rings.

Metallocyclic Chain Structures. As determined by single-crystal analysis, the coordination polymer **3** exhibits metallocyclic chain architecture in the solid state. This structure is quite different from **2**, despite the fact that compounds **2** and **3** are prepared from the same reaction as a mixture. As shown in Figure 10, each copper center of **3** lies in an octahedral (CuN$_4$O$_2$) coordination geometry, with four equatorial pyridyl nitrogen donors from four **L1** ligands and with the axial positions being occupied by two oxygen atoms from two crystallographically equivalent nitrate ions. The Cu−N bond lengths are 2.022(2) and 2.044(2) Å, respectively, which are comparable to the corresponding bond distances of **2**. The Cu−O bond distance is 2.471(2) Å, which is longer than that found in **2**. The dihedral angle between the terminal pyridyl groups is 90 °C, which is, presumably, because of the steric interactions of the spacer benzene rings. As shown in Figure 10, the orientation of the terminal nitrogen donors on the 3-pyridyl rings are different from those in **2**, although the building block of **3** exhibits an X-shaped arrangement.

The architectural pattern of **3** demonstrates a 1D chain motif composed of copper centers linked together via the four crystallographically equivalent **L1** ligands. The individual links in the chains consist of macrocyclic Cu$_2$(**L1**)$_2$ units, which can be viewed as 30-membered macrocycles enclosing the two Cu(II) atoms and two **L1** ligands (Figure 11). The approximate dimensions of the rings are 16 × 6 Å.[68] The intrachain Cu···Cu separation is 16.454 Å. The nitrate ions are located on both sides of the Cu$_2$(**L1**)$_2$ ring planes. Interestingly, there are two sets of 1D chains in **3**. Each set stacks together in a face-to-face fashion to generate

(68) The pore dimensions described here are crystallographically scalar quantities and do not account for the van der Waals radii of the atoms defining the pore.
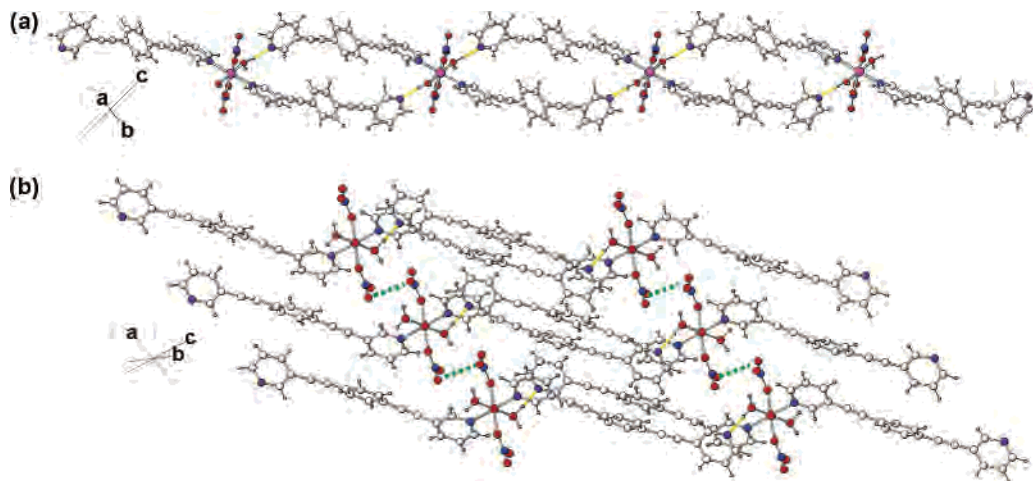
Figure 9. Hydrogen-bonding interactions of the dinuclear compound **5**. (a) Hydrogen bonds between the dinuclear units are shown as yellow lines. (b) Additional hydrogen bonds between coordinated water molecules and the nitrate anions (black dotted lines H···O = 2.270(1) Å and = 2.548(1) Å) and between the nitrate ions (green dotted lines O···O = 2.922 Å).
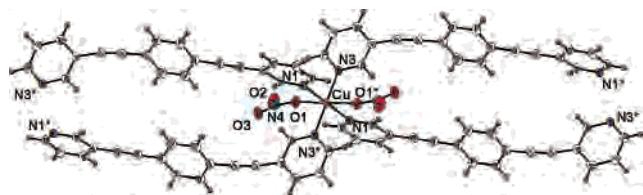
Figure 10. (CuN$_4$O$_2$) coordination environment of **3**, drawn with 50% probability ellipsoids. The Cu atom resides on a crystallographic inversion center.

elliptical channels along the crystallographic [111] direction, as shown in Figure 11. The interchain Cu···Cu contact is 8.728 Å. A few weak interchain interactions between nitrate ions and between benzene spacers contribute significantly to the structural organization of **3** in the crystalline phase.

Polycatenated Ladder Structure. Single-crystal X-ray analysis of compound **6** showed that two independent Co atoms reside in heptahedral (Co1) and octahedral (Co2) environment, with two pyridyl groups at the axial positions and one pyridyl group at the equatorial position, giving rise to a T-shaped arrangement at the metal center (Figure 12).[69] The nitrate groups are practically symmetrically chelating and show significant asymmetric Co—O bond interactions.[70] The building block of **6** is composed of a T-shaped arrangement giving rise to a one-dimensional ladder. Simple molecular ladders composed of T-shaped metal centers are common structural motifs for M(NO$_3$)$_2$ salts and long, rigid bidentate spacer ligands with a metal-to-ligand ratio of 2:3.[71] However, the most interesting structural feature of **6** consists of mutually twofold interpenetration of the ladders that gives a catenation to each other with 3D architecture, schematically illustrated in Figure 13. This arises from the fact that there

are two distinct sets of ladders running in two different directions ([112] and [1−12]), and the ladders of one set are catenated to those of the other set and vice versa. Each square grid of a given ladder is interlocked with two squares of two adjacent ladders of the other set; thus the polycatenation within a 1D motif increases the dimensionality of the whole polymeric system. Thus, a 1D→2D dimensional increase can be achieved by parallel catenation, whereas a 1D→3D dimensional expansion inevitably results from inclined catenation. Most of the known 1D→3D transformations are created by twofold inclined catenation, where each square is interlocked by the other two ladders.[56−59,71] A closely related example of **6** that exhibits a 3D polycatenated assembly has been reported by Fujita in 1995,[59] where the interpenetration was perpendicular to the orientation of the original ladder and four ladders, instead of two, catenate each.

Noninterpenetrating Square-Grid Structure. A view depicting the pseudooctahedral 4 + 2 coordination environment at the cadmium(II) center is shown in Figure 14a. Four crystallographically equivalent ligands of **L2** are situated in a square planar fashion about the Cd center (Cd—N(1) = 2.318(2); N(1)—Cd—N(1)* = 148.45° and Cd—N(2) = 2.375(2) Å; N(2)—Cd—N(2)* = 164.05°); while two crystallographically equivalent nitrate ions (Cd—O(1) = 2.563(2) Å and Cd—O(3) = 2.667(2) Å) occupy the axial positions. The pyridyl rings and benzene spacer of each ligand are twisted relative to one another. Moreover, the ligands demonstrate nonlinearity, which can clearly be seen in Figure 14b. The curvature and presence of the spacer benzene ring of ligand **L2** leads to an open-grid space, in particular, the ligand orientation alternates with the benzene group rotated by approximately 60° on the opening side of each grid, projecting the side chain alternately parallel and perpendicular to the plane of the grid. The noninterpenetrating square-grid polymeric structure of **7** generated from such coordination consists of the familiar two-dimensional square-grid type layers, in this case with inner square cavity dimensions of 20.6 × 20.4 Å^2, comparable to those of related com-

(69) The geometry of the pyridyl groups around the two individual cobalt(II) atoms deviates from the ideal T-shape cobalt complexes as follows: Co1—N1 = 2.131 Å; Co1—N2 = 2.131 Å; Co1—N3 = 2.149 Å; Co2—N6 = 2.147 Å; Co2—N7 = 2.119 Å; Co2—N8 = 2.142 Å.

(70) The bond lengths of asymmetric Co—O are as follows: Co1—O1 = 2.129 Å; Co1—O3 = 2.382 Å; Co1—O4 = 2.178 Å; Co1—O5 = 2.259 Å; Co2—O7 = 2.130 Å; Co2—O10 = 2.194 Å.

(71) Carlucci, L.; Ciani, G.; Proserpio, D. M. *J. Chem. Soc., Dalton Trans.* **1999**, 1799−1804.
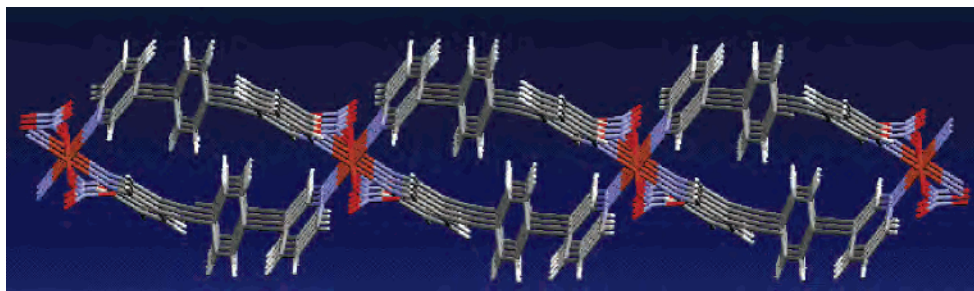
Figure 11. View of macrocycle chain architecture of **3**. Each of the macrocycles stacks along the crystallographic [111] direction and creates elliptical channels.
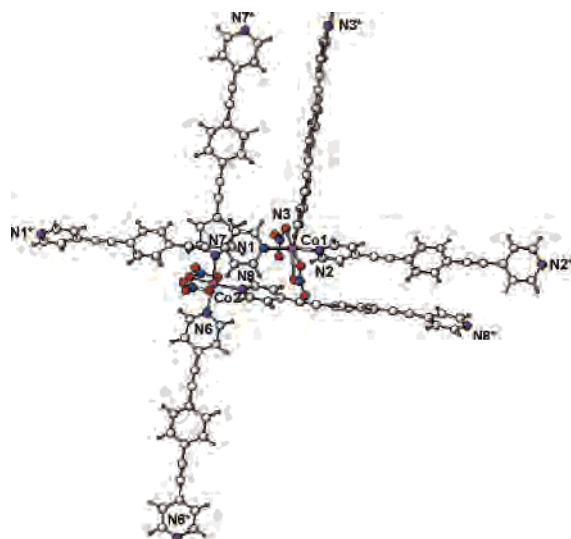

Figure 12. Two independent T-shaped arrangements in **6**, drawn with 50% probability ellipsoids. Co1 atoms reside in heptahedral and Co2 in octahedral environment.

pounds[3,45,72] but, on the other hand, larger than that generated from 4,4′-bipyridine with similar metals (Zn, Ni, Cu, Cd).[58,73,74] The grids are stacked in an ABAB fashion that creates rectangular channels of dimension 20 × 11 Å² (Figure 15a), thus reducing the accessible porosity of the grids, which is reflected in a greatly diminished solvent-accessible volume in the unit cell. The adjacent stacked grids are not planar because of the deformation of the **L2** ligand, and in Figure 15b this undulation can clearly be seen. The closest contacts between the nitrate ion and benzene spacer (O···H−C) of the adjacent layers is 2.570 and 3.293 Å. Thus, the use of the long ligand **L2** has afforded a new noninterpenetrating square-grid structure (**7**), with large guest-free infinite channels, while the porosity of the framework is very close to that of the recent noninterpenetrating grid structure reported by Fujita using a longer ligand, namely, [{Ni(4,4′-bis(4-pyridyl)biphenyl))₂(NO₃)₂·4o-xylene}ₙ].[45]

Linear Chain Structure. The repeat unit of the polymeric compound **8** is shown in Figure 16. The copper atom is in a six-coordinate 4 + 2 pseudooctahedral geometry defined by two nitrogen donors from two *trans*-**L2** ligands and four

oxygen donors from two hfca chelating ligands. This arrangement is quite similar to the geometry of the copper centers found in Cu(hfac)₂(pyrazine)₂[74] [Cu(hfac)₂{1,2bis-(4-pyridyl)ethane}]ₙ[74] and Cu(hfac)₂{3- and 4-(*N*-oxyl-*trans*-butylamino)-pyridines}₂.[75] The Cu−N bond lengths in **8** are 2.024(1) Å and 2.043(1) Å, which are slightly longer than those in the similar polymeric compounds previously reported, such as [Cu(hfac)₂{1,2bis(4-pyridyl)ethane}]ₙ [Cu−N, 2.014(7) Å] and [Cu(hfac)₂{4,4′-trimethylenebipyridine}]ₙ [Cu−N, 1.992(6) and 2.017(6) Å].[74] The Cu−O bond lengths in **8** are 2.027(2) and 2.240(2) Å, where Cu−O(1) is significantly shorter than Cu−O(2). Similar differences can also be found in other cis coordinated Cu(II) complexes[75] [Cu−O, 2.019(8) and 2.327(10) Å].

Each copper center is connected through the pyridyl nitrogen atoms of the **L2** ligands into a 1D linear chain along the crystallographic *b*-axis. Interestingly, three sets of distinct 1D linear chains, denoted as A, B, and C in Figure 17, run through the *bc*-plane. Moreover, these chains are associated by close contacts into AC and BC pairs to increase the dimensionality of the supramolecular network. Figure 18a shows the linking mechanism between the fluorine atoms and the benzene rings (F···H−C = 2.649 and 2.927 Å) of two crystallographically equivalent A and C chains running perpendicular to the *c*-axis. In addition, Figure 18b shows the linking between the oxygen atoms from hfac and hydrogen atoms from the pyridyl rings (O···H−C = 2.487 and 2.812 Å) within two crystallographically equivalent A and C chains lying along the *b*-axis. In this compound, the intrapolymer and the closest interpolymer Cu···Cu distances are 20.565 and 6.476 Å, respectively. To the best of our knowledge, this interpolymer distance is the shortest distance among polymers constructed from Cu(hfac)₂. Moreover, the three distinct linear chain motifs in the same coordination polymer is also rare.[41,64−66,77,78]

Thermogravimetric Analysis. To investigate the thermal stability of the framework of compounds **1**−**8**, thermogravimetric analyses (TGA) were performed on samples consisting of numerous single crystals of each compound. Compounds

(72) Biradha, K.; Fujita, M. *J. Chem. Soc., Dalton Trans.* **2000**, 3805−3810.

(73) MacGillivray, L. R.; Groeneman, R. H.; Atwood, J. L. *J. Am. Chem. Soc.* **1998**, *120*, 2676−2677.

(74) Biradha, K.; Mondal, A.; Moulton, B.; Zaworotko, M. J. *J. Chem. Soc., Dalton Trans.* **2000**, 3837−3844.

(75) Dong, Y.-B.; Smith, M. D.; Layland, R. C.; zur Loye, H.-C. *Inorg. Chem.* **1999**, *38*, 5027−5033.

(76) Ishimaru, Y.; Kitano, M.; Kumada, H.; Koga, N.; Iwamura, H. *Inorg. Chem.* **1998**, *37*, 2273−2280.

(77) Kamiyama, A.; Noguchi, T.; Kajiwara T.; Ito, T. *Inorg. Chem.* **2002**, *41*, 507−512 and references cited therein.

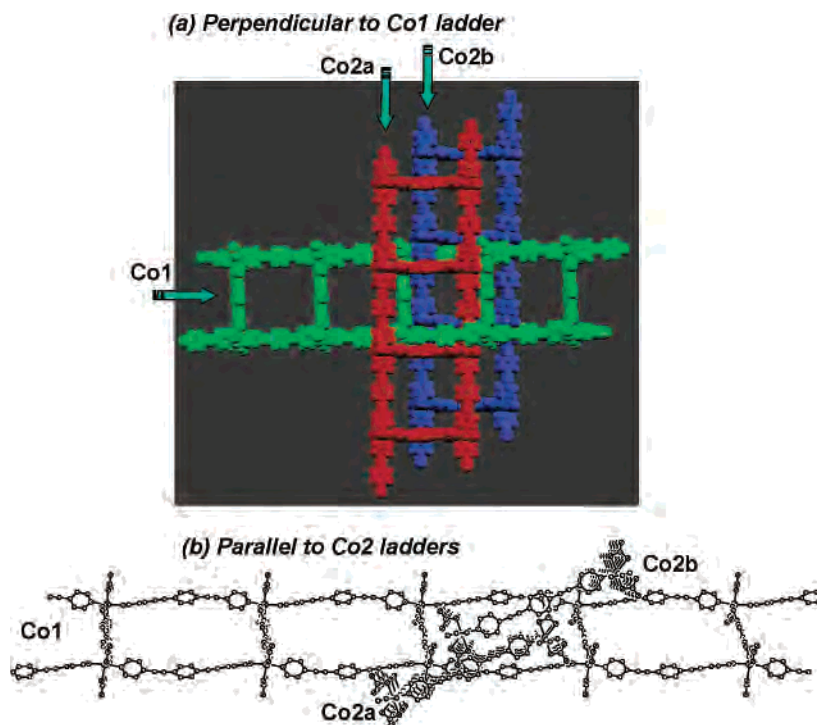(78) Tabellion, F. M.; Seidel, S. R.; Arif, A. M.; Stang, P. J. *Angew. Chem., Int. Ed.* **2001**, *40*, 1529−1532.

Figure 13. Perspective view of two independent one-dimensional ladder architectures of **6**, forming an interpenetrating polycatenated assembly. The structural view is simplified (a) perpendicular to the Co1 ladder and (b) parallel to Co2 ladders.
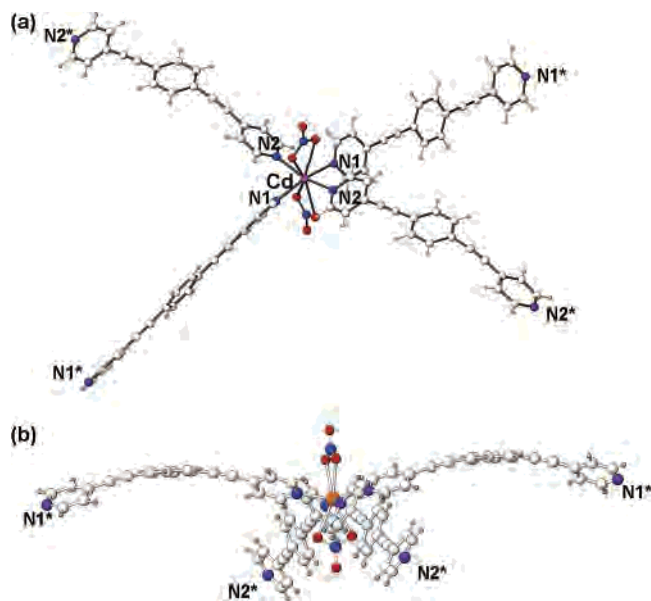

Figure 14. (a) The local coordination environment around the Cd atom in **7** is shown with the selected atomic numbering scheme. (b) The nonlinearity and twisting features of the ligands is shown here. Ellipsoids are shown at the 50% probability level.

1−**5** and **8** were heated under nitrogen flow, whereas **6** and **7** were heated in a helium atmosphere. The single crystalline performance of compounds **1**−**3** collapsed at room temperature because of immediate removal of solvent from the crystals. Because of the facile loss of solvent from these compounds, initially the samples were brought to ∼50 °C to remove the solvents, held at this temperature until a stable weight was achieved, after which time the heating was resumed. In the temperature range of 230−268 °C, **1** underwent complicated multiple weight loss steps, with the
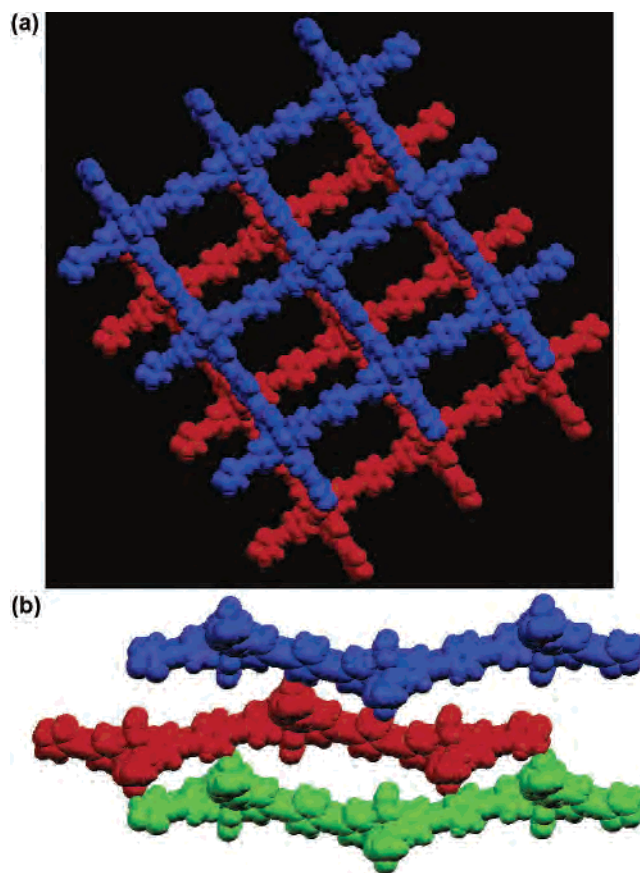

Figure 15. Noninterpenetrating square-grid structure (**7**). (a) Stack of three square-grid layers (the blue layer overlaps with the green layer and is not visualized in the diagram). The grids stack in an ABAB fashion, creating large infinite channels of dimensions 20 × 11 Å². (b) A view parallel to three adjacent stacked grids shows that the grids are not planar but undulate.
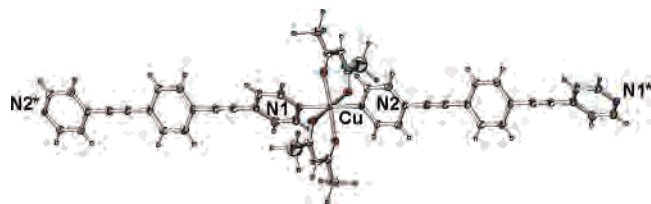
Figure 16. The local coordination environment around the Cu atom in **8** is shown with the selected atomic numbering scheme. Ellipsoids are shown at 50% probability level.

total loss corresponding to one ligand (**L1**) and one nitrate ion (obsd 59.00%, calcd 58.89%). The TGA data for **2** show that the first weight loss (11.88%) occurs at 160 °C, corresponding to the loss of two molecules of methanol solvent (calcd 12.46%). The framework apparently collapses because of the release of one ligand and a nitrate ion per formula unit, which occurs between 250 and 284 °C with an observed weight loss of 51%. Compound **3** is a minor product from **2** and is an insufficient quantity to examine TGA analysis. A single-step weight loss was observed in compound **4**, and the final product is black and amorphous.

The weight loss from 228 to 260 °C is believed to be due to the loss of the **L1** and hfac ligands, which is quite typical for organic−inorganic coordination polymers consisting of Cu(hfac)$_2$ cations and *N,N'*- bidentate-type ligands. In compound **5**, the first weight loss from 150 to 170 °C corresponds to the loss of the one water. Finally, the compound is accompanied by the decomposition from 350 to 470 °C, corresponding to the remaining **L1** ligands and nitrate ions. In compound **6**, the framework is stable up to 260 °C. The poorly defined weight loss, between 65 °C and 155 °C, is due to the loss of solvent. Starting around 260 °C, the **L2** ligands and nitrate ions decompose and leave a black solid behind. The TGA data of compound **7** suggests that the square-grid frameworks are thermally stable up to 220 °C. The massive weight loss in the 220−380 °C range is indicative of sample decomposition. As expected, the thermal stability of compound **8** is quite similar to that of compound **4**. A broad weight loss occurs essentially from 260 to 296 °C, corresponding to removal of the **L2** and hfac ligands.
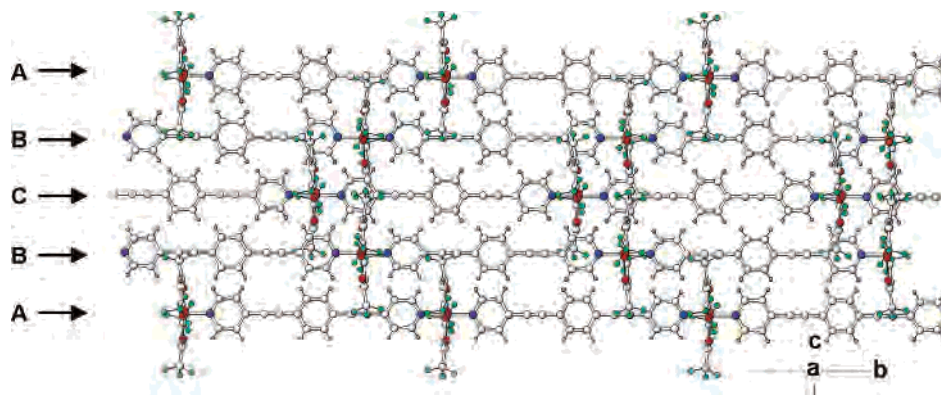

Figure 17. View of the crystallographic *bc*-plane in **8** where three distinct one-dimensional linear chains are in a parallel fashion and are denoted as chain-A, chain-B, and chain-C.
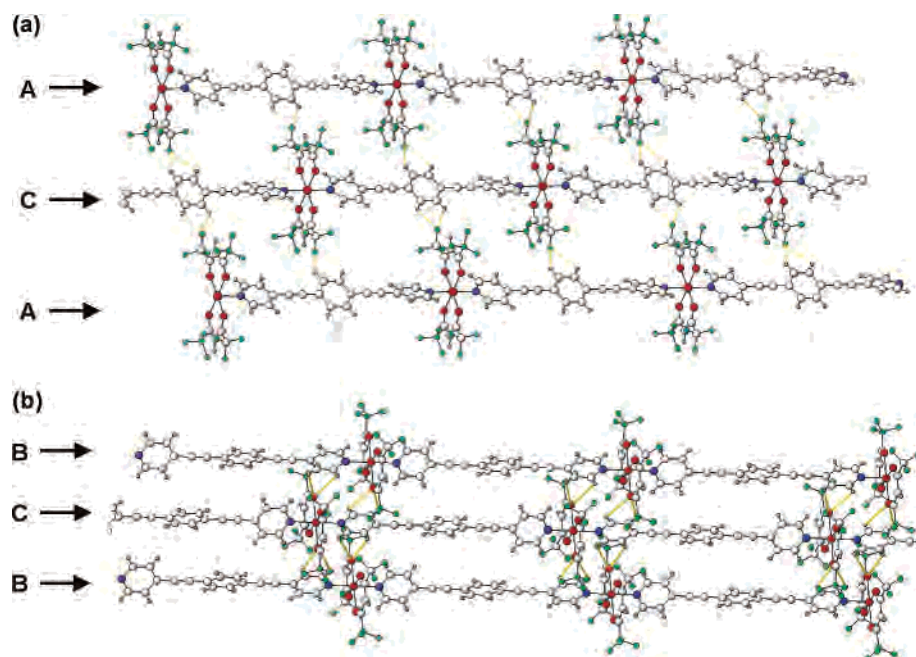

Figure 18. Yellow lines indicate hydrogen-bonded interactions between chains (a) A and C and (b) B and C.

Conclusion

The ligands **L1** and **L2** have yielded numerous polymeric structures with common metal−nitrate and metal−hexafluoroacetylacetonato salts. The coordination arrangements of the **L1** ligand result in some interesting features, such as coordination environments leading to several novel zigzag chain architectures in Cd(II), Co(II), and Cu(II) systems. These chains are additionally hydrogen-bonded via coordinated nitrate, solvent, and water molecules to create two- or three-dimensional frameworks. The copper nitrate forms two different structures in the same reaction mixture, and these structural features are primarily influenced by the coordination environment of the metal center. The **L1** ligand can also be successfully reacted with copper bis(hexafluoroacetylacetonato) to yield novel three-dimensional polymers. In contrast, **L2** coordination polymers form one-dimensional linear chain architectures with copper bis(hexafluoroacetylacetonato) salts, where three distinct chains are closely linked with the metal center and the atoms from the ligand to build a bundle of chains. Both **L1** and **L2** coordinated to Cu(hfac)$_2$ are comprised of a trans occupied coordination sphere, and their structural motif depends on ligand orientation as well as intermolecular interactions between adjacent ligands. The reaction of the metal nitrates with the **L2** ligand have resulted in four remarkable framework structures. It is interesting that Cd(II), Co(II), and Cu(II) nitrates afford infinite cyclic systems: (i) noninterpenetrating square grid, (ii) interpenetrating polycatenane ladder frameworks, and (iii) infinite ladders interpenetrated by infinite chains, respectively.[79]

The 10 frameworks described in this paper are the first reported examples of extended coordination polymers incorporating the **L1** and **L2** ligands. These polymers illustrate the propensity by which these metal−ligand systems adopt chain- and ringlike architectures, even when containing dramatically nonlinear bridging ligands. We have demonstrated the manner in which two different orientations of the pyridyl nitrogen atoms can strongly bind to the nitrate salts of Cd(II), Co(II), Cu(II), and Cu(hfac)$_2$ to form these crystalline polymeric compounds (**1**−**10**). The results presented in this article not only include diverse structural motifs but also highlight the usefulness of the two different nitrogen positions of the pyridyl ligands and the potential for obtaining novel supramolecular architectures on the basis of similar components.

Supporting Information Available: X-ray crystallographic data (CIF files) for **1**−**8**. This material is available free of charge via the Internet at http://pubs.acs.org.

IC050080D

---

(79) The structures (**9** and **10**) from copper nitrate are reported in our preliminary communication and are not described here. See ref 47.